International Journal of Technology

http://ijtech.eng.ui.ac.id

Research Article

Tailoring Crosslinked Polyurethane–Acrylate Hybrid Networks Using a High Isocyanate-polyol ratio (NCO/OH) Ratio for Improved Adhesion and Durability

Aidana B. Arystan[1*], Maratbek T. Gabdullin[1], Khaldun M. Al Azzam[2], Lyazzat Bekbayeva[3], Rinat Zhanibekov[1], Mohamad Nasir Mohamad Ibrahim[4], El-Sayed Negim[1], Eny Kusrini[5,6,7]

[1]School of Materials Science and Green Technologies, Kazakh British Technical University, St. Tole bi 59, 050000, Almaty, Kazakhstan

[2]Department of Chemistry, Faculty of Science, The University of Jordan, 11942, Amman, Jordan

[3]National Nanotechnological Laboratory of Open Type, Al-Farabi Kazakh National University

[4]Materials Technology Research Group (MaTRec), School of Chemical Sciences, Universiti Sains Malaysia, 11800 Minden, Penang, Malaysia

[5]Department of Chemical Engineering, Faculty of Engineering, Universitas Indonesia, Kampus Baru UI, Depok 16424, Indonesia

[6]Green Product and Fine Chemical Engineering Research Group, Laboratory of Chemical Product Engineering, Universitas Indonesia, Kampus Baru UI, Depok, 16424, Indonesia

[7]Advanced Materials Research Center, Faculty of Engineering, Universitas Indonesia, Kampus Baru UI, Depok, 16424, Indonesia

[*]Corresponding author: Aidanaarystan94@gmail.com; Tel.: +77029850094

Abstract: Polyurethane acrylate hybrid coatings have attracted significant attention for protective applications; however, the influence of high NCO/OH ratios and polyol architecture on their performance remains insufficiently explored. Polyurethane/2-hydroxy-1-methylethyl acrylate (PUA/HMEA) hybrid resins were synthesized via a polyaddition reaction using hexamethylene diisocyanate and mixed polyols (GP-2000 and GP-4000) at a relatively high NCO/OH ratio of 2.5. The hybrid network structure was confirmed by FTIR analysis. The effect of HMEA incorporation on rheological, mechanical, adhesion, and chemical resistance properties was systematically investigated. The results revealed a significant enhancement in performance with increasing HMEA content, achieving a tensile strength of up to 205 MPa, adhesion strength of 10.5 MPa, and a contact angle of 153°, indicating improved mechanical integrity and surface hydrophobicity. Furthermore, the hybrid coatings exhibited superior resistance to water, solvents, and corrosive environments. These improvements are attributed to the formation of a highly crosslinked network resulting from the combination of a high NCO/OH ratio and reactive acrylate functionality. The findings demonstrate that tailoring network structure through controlled formulation provides an effective strategy for designing high-performance polyurethane–acrylate coatings for demanding industrial applications.

Keywords: Acrylic; Coating; Corrosion; Hybrid; Polyurethane

1. Introduction

Polyurethanes (PUs) comprise a diverse class of advanced polymer materials that are extensively applied across industrial sectors, such as surface coatings, bonding agents, elastomeric systems, and foam-based products. Their extensive adoption is primarily driven by their outstanding mechanical robustness, flexibility, wear resistance, and strong adhesive interactions with diverse substrate surfaces (Amini et al., 2025; David et al., 2023; Kim et al., 2026; Liu et al., 2026). The physicochemical properties of polyurethane materials can be tailored over a

https://doi.org/10.14716/ijtech.v17i4.8408
Received February 2026; Revised February 2026; Accepted May 2026

wide range to meet the requirements of specific applications by selecting different combinations of diisocyanates and polyols (Maamoun et al., 2025; Maurya et al., 2023; Shuang et al., 2025). In general, diisocyanates contribute to the formation of hard segments within the polyurethane backbone, imparting mechanical strength, whereas the soft segments derived from polyols are primarily responsible for flexibility and toughness (Asensio et al., 2023; Kim et al., 2016). Thus, the ratio between rigid and flexible blocks has a decisive effect on the final properties of the blocks (Dall'Agnol et al., 2021). Despite their many advantages, polyurethanes have several disadvantages that limit their use in certain cases. These include limited heat resistance, low rigidity, and high sensitivity to moisture, especially when exposed to high temperatures or aggressive environments (Breheny et al., 2025; Oladele et al., 2025; Pooneh & Reza, 2026).

Therefore, there is growing interest in developing polyurethane-acrylate (PU-A) hybrids that combine the advantageous properties of both polymer types (Keskin et al., 2025). Acrylic components contribute to alkali resistance, weather durability, improved pigment dispersion, and cost efficiency, while the polyurethane phase imparts enhanced toughness, flexibility, and superior film-forming characteristics (Azani & Hassanpour, 2024; Negim et al., 2024a; Negim et al., 2024b; Zhou et al., 2024). Secondly, chemical bonding of two types of polymers allows the formation of a homogeneous and stable product, as opposed to simple blends, where incompatibility between polyurethane and acrylic phases causes phase separation during processing that affects performance (Allami et al., 2021; Keskin et al., 2025; Manas, 2024; Peruzzo et al., 2011; Puyadena et al., 2022; Shafeeq & Unnikrishnan, 2020; Su et al., 2024). In addition, polyurethane-acrylate (PU-A) hybrids benefit from the combination of rapid radical polymerization of acrylate double bonds and step-growth polymerization of urethane linkages (Suwen et al., 2022).

Within these hybrid materials, the acrylate segment promotes fast curing through free-radical polymerization, whereas the polyurethane phase undergoes curing via polyaddition reactions between isocyanates and polyols, resulting in a crosslinked network that combines flexibility with long-term durability. This dual-curing behavior contributes to improved mechanical performance and helps reduce the brittleness commonly observed in fully acrylated systems (Kozakiewicz, 2016; Shimin et al., 2024). As a result, polyurethane–acrylate (PU–A) hybrids with UV-curable characteristics have been widely developed, as they combine the rapid curing of acrylate groups under ultraviolet irradiation with the strength, flexibility, and long-term durability provided by the polyurethane segments (Aizpurua et al., 2020; Dall'Agnol et al., 2021; Guo et al., 2024; Niu & Bian, 2012; Xu et al., 2012).

The weight ratio between the polyurethane and acrylic phases strongly influences the performance of polyurethane–acrylate (PU–A) hybrid materials (Kim et al., 2026). Therefore, considerable attention has been paid to optimizing this ratio to achieve a suitable balance among mechanical strength, durability, and processability, particularly for coating applications. One study (Byczyński et al., 2024; Son et al., 2011) reported that increasing the acrylic monomer content improved hardness, water resistance, and tensile yield strength; however, this was accompanied by a reduction in abrasion resistance and flexibility, with an acrylic content of 30 wt% identified as the optimal compromise between these properties. Peruzzo et al. (2010) observed that the mechanical properties of hybrids prepared by seeded emulsion polymerization remained relatively unchanged up to an acrylic content of 50 wt%, beyond which a marked decrease in tensile strength occurred. This finding underscores the importance of defining a maximum acrylic content that preserves performance while controlling material costs. Similarly, another study demonstrated that an optimized PU/acrylic ratio resulted in the highest hardness and chemical resistance, whereas further increases in the acrylic fraction led to a noticeable deterioration in overall performance (Zhang et al., 2025).

Despite extensive studies on polyurethane–acrylate hybrid materials, most previous work has primarily focused on optimizing the composition ratio between polyurethane and acrylic phases, while the combined influence of elevated NCO/OH ratio and mixed polyol molecular architecture remains insufficiently explored. Therefore, the present study investigates the effect

of a relatively high NCO/OH ratio (2.5), GP-2000/GP-4000 mixed polyols, and varying HMEA incorporation on the structure–property relationships of polyurethane acrylate hybrid coatings. To establish an effective formulation strategy for advanced protective coatings, the prepared materials were characterized by FTIR spectroscopy, rheological measurements, adhesion testing, mechanical performance, wettability, and chemical resistance evaluation.

2. Experimental

2.1 Materials

Polypropylene glycol GP-2000 (M_w = 2000 g/mol, hydroxyl number = 56 mg KOH/g) and GP-4000 (M_w = 4000 g/mol, hydroxyl number = 29.5 mg KOH/g) were supplied by Korea PTG (South Korea). Both polyols were dried at 80°C under reduced pressure (1–2 mm Hg) for 2 h before use. Dibutyltin dilaurate (DBTDL) and hexamethylene diisocyanate (HDI) were obtained from Bayer AG (Germany). 2-Hydroxy-1-methylethyl acrylate (HMEA) was purchased from Sigma. No additional purification or pretreatment of HMEA was required, as it was used for coating applications rather than medical purposes.

2.2 Synthesis and Structural Characterization of PUA and PUA/HMEA

The polymerization process was performed in a 500 mL separable four-neck round-bottom reactor equipped with mechanical agitation, temperature monitoring, and a moisture-trapping tube-fitted condenser. To maintain a stable reaction temperature, all reactions were conducted under an inert nitrogen atmosphere using an oil bath. The nitrogen flow rate was maintained at approximately 25 mL min^{-1} throughout the reaction to minimize moisture ingress and maintain an inert environment. The stirring speed was fixed at 500 rpm to ensure homogeneous mixing of the reaction components. Reaction progress was monitored by periodic determination of residual isocyanate content using the di-n-butylamine titration method, and the reaction endpoint was considered achieved when the measured %NCO matched the theoretical value within ±0.2%.

For the synthesis of PUA, hexamethylene diisocyanate (HDI, 13.1%) and the polyols (85.9%) were first introduced into the reactor and allowed to react at 90°C for 3 h until the calculated NCO content was attained, as verified by the di-n-butylamine titration method, maintaining an NCO/OH ratio of 2.5. HDI, polyols, and HMEA in various proportions were simultaneously added to the reactor and subjected to the same reaction conditions (90°C, 3 h) until the calculated isocyanate (NCO) content was attained for the preparation of PUA/HMEA hybrid resins. The reaction pathways for PUA and PUA/HMEA formation are presented in Figure 1, and the prepared samples with varying HMEA concentrations are listed in Table 1.

The formation of polyurethane networks proceeds via a step-growth polyaddition reaction between the isocyanate (–NCO) groups of HDI and the hydroxyl (–OH) groups of the polyols, resulting in the formation of urethane linkages (–NH–CO–O–). The hydroxyl group of 2-hydroxy-1-methylethyl acrylate (HMEA) also reacts with isocyanate groups in the case of PUA/HMEA hybrid systems, leading to the incorporation of acrylate functionalities into the polymer backbone. The presence of both urethane linkages and pendant acrylate groups enables the formation of a crosslinked hybrid network, which contributes to enhanced mechanical and chemical resistance (Kozakiewicz, 2016; Negim et al., 2020; Xu et al., 2012).

2.3 Film Preparation

The resin blended with dibutyltin dilaurate (DBTDL) at 1 wt% relative to PUA produced PUA films. In contrast, PUA/HMEA films were obtained by incorporating benzoyl peroxide (BPO) at 1 wt% based on the PUA/HMEA content, followed by casting the mixtures onto a level surface. The films were cast to obtain a dry film thickness of 75 ± 5 µm. The coatings were then allowed to cure at room temperature for 5 days. After curing, the films were kept in a desiccator at ambient temperature until subsequent characterization and testing.

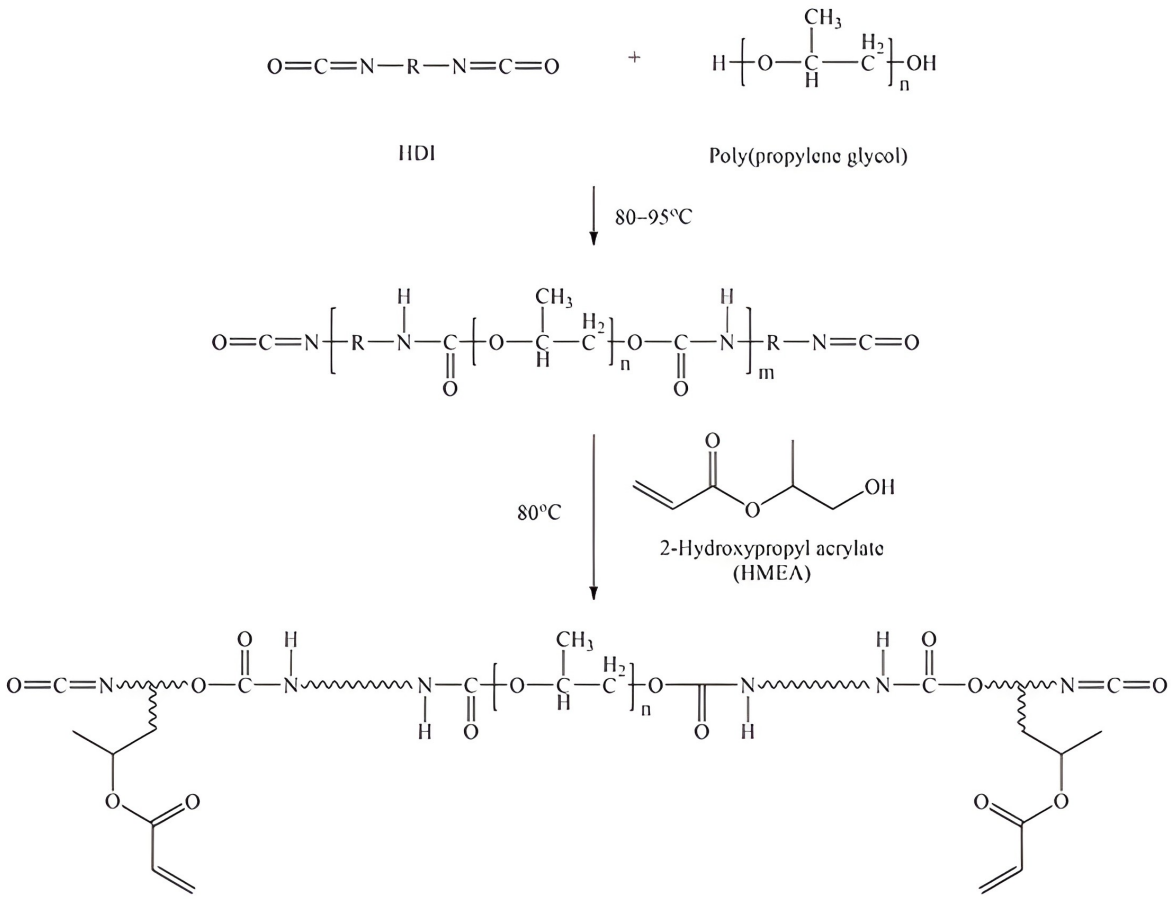

Figure 1 Proposed synthesis route for PUA and PUA/HMEA hybrid networks through HDI polyaddition with GP-2000/GP-4000 polyols, followed by HMEA incorporation to introduce pendant acrylate functionality and enhance crosslink density

Table 1 Feed compositions of PUA and PUA/HMEA systems

Samples	PUA Wt (%)	PUA/HMEA Wt (%)		
		PUA/3 HMEA	PUA/6 HMEA	PUA/12 HMEA
GP 2000	37.26	7.10	10.70	18.10
GP 4000	48.68	71.60	54.64	21.25
HMEA	**0.00**	**3.01**	**6.25**	**12.84**
HDI	13.10	18.70	28.38	47.83
NCO/OH	2.50	2.50	2.50	2.50

2.4 Tests

Fourier-transform infrared (FTIR) spectra were recorded using a Bruker Tensor 37 FTIR spectrometer. The viscosities (η) of the polyurethane (PU), acrylate (AC), and PU/AC hybrid systems were measured using a Brookfield viscometer equipped with Spindle 2, which operated at rotational speeds of 5 and 50 rpm at 25°C following ASTM D2196. Two rotational speeds (5 and 50 rpm) were selected to evaluate the samples' shear-dependent flow behavior. The lower speed (5 rpm) represents low-shear conditions, while the higher speed (50 rpm) simulates higher shear conditions typically encountered during brushing or coating applications. Comparing viscosity at these two shear rates allows the assessment of the system's non-Newtonian behavior. The thixotropy index (TI) is defined as the ratio of viscosity measured at low shear rate to that

measured at high shear rate (η_5/η_{50}). It is used to quantify the shear-thinning behavior of the material. A higher TI value indicates stronger thixotropic behavior, indicating that the material exhibits a significant decrease in viscosity under shear and recovery upon rest.

The thixotropy index was calculated using Equation (1):

$$\mathrm{TI} = \frac{\eta_5}{\eta_{50}} \tag{1}$$

The water contact angles on the sample surfaces were determined using a CAHN DCA-322 contact angle analyzer following ASTM D73334. Measurements were conducted using distilled water at 25°C, with a drop deposition rate of 100 µm s^{-1}. A single water droplet was placed onto the surface of each sample using a microsyringe, and the contact angle was determined by monitoring the droplet profile on the instrument display. The reported contact angle values are the mean of three measurements performed at different positions on each film surface.

The tensile behavior of the cast films was determined using an MTS 10/M universal testing machine at a crosshead speed of 50 mm min^{-1}. A minimum of four specimens were tested for each formulation, and average values were calculated using a 1 kN load cell. Surface hardness was evaluated using an indentation-type Barcol hardness tester according to ASTM B648-10. Pull-off tests conducted according to ASTM D4541 measured the adhesion of the hybrid polymer coatings to metal substrates.

For the corrosion resistance test, uniform substrate conditions were achieved using standardized steel test panels cleaned with acetone according to ASTM D6386. Coatings were applied with a spiral bar applicator set to create a 150 µm wet film thickness, following ASTM D823 guidelines. After application, the panels were cured at room temperature for one week before testing. The dry film thickness was checked with an elcometer based on ASTM D7091 and kept within 50 ± 5 µm. The corrosion resistance of the coated panels was evaluated by immersing them in saline (10% NaCl), alkaline (10% NaOH), acidic media (37% HCl and H_2SO_4), and water, following the appropriate ASTM G31 standard procedures. Solvent resistance was evaluated using xylene, methyl ethyl ketone (MEK), and ethanol according to ASTM D5402-93, while water resistance was tested according to ASTM D1647-89. All dry time measurements were recorded at 25°C.

3. Results and Discussion

3.1 FTIR Analysis

The chemical structures of the PUA and PUA/HMEA hybrid resins were examined using FTIR spectroscopy. As shown in Figure 2, the FTIR spectrum of the typical PUA resin exhibits characteristic absorption bands at 2900–2870 cm^{-1} corresponding to aliphatic $–CH_2$ and $–CH_3$ stretching vibrations, a distinct band at 2251 cm^{-1} attributed to the isocyanate (NCO) group, and a band at 1091 cm^{-1} associated with the C–O–C stretching vibration (Kozakiewicz, 2016; Shafeeq & Unnikrishnan, 2020).

In contrast, the FTIR spectra of the PUA/HMEA hybrids display the emergence of additional absorption peaks at 1719 cm^{-1}, assigned to the carbonyl (C=O) group, as well as bands at 1644 cm^{-1} and 1102 cm^{-1} corresponding to the stretching vibrations of the C=C bond and C–O–C linkage, respectively (Figure 2). The observed carbonyl (C=O), vinyl (C=C), and ether (C–O–C) bands are in good agreement with the reports on polyurethane–acrylate hybrid systems, confirming the successful incorporation of acrylate functionalities into the polymer network (Puyadena et al., 2022; Xu et al., 2012). These new peaks confirm the successful incorporation of HMEA into the polyurethane network through its reaction with HDI. Furthermore, a noticeable reduction in the intensity of the NCO absorption band at 2251 cm^{-1} is observed, which can be attributed to the reaction between the hydroxyl groups of HMEA and the isocyanate groups of HDI.

The reduction in the NCO band intensity confirms the progressive consumption of free isocyanate groups. Simultaneously, increased carbonyl band intensity indicates urethane linkage

formation. These spectral changes support increased network formation with the incorporation of HMEA.

A semi-quantitative interpretation of the FTIR spectra further supports the progress of the polyaddition reaction. The decrease in the relative intensity of the NCO absorption band at 2251 cm^{-1} together with the increased intensity of the carbonyl (C=O) band near 1719 cm^{-1} indicates the progressive consumption of isocyanate groups and the formation of additional urethane linkages within the hybrid polymer network. The decrease in NCO band intensity, along with the appearance of acrylate-related peaks, confirms the reaction between isocyanate groups and HMEA, indicating the formation of a chemically bonded hybrid network rather than a physical blend (Negim et al., 2024a; Su et al., 2024). These spectral changes provide indirect evidence of an increased degree of crosslinking after HMEA incorporation into the polyurethane matrix. Figure 1 shows the proposed chemical structures of PUA and the PUA/HMEA hybrid resins.

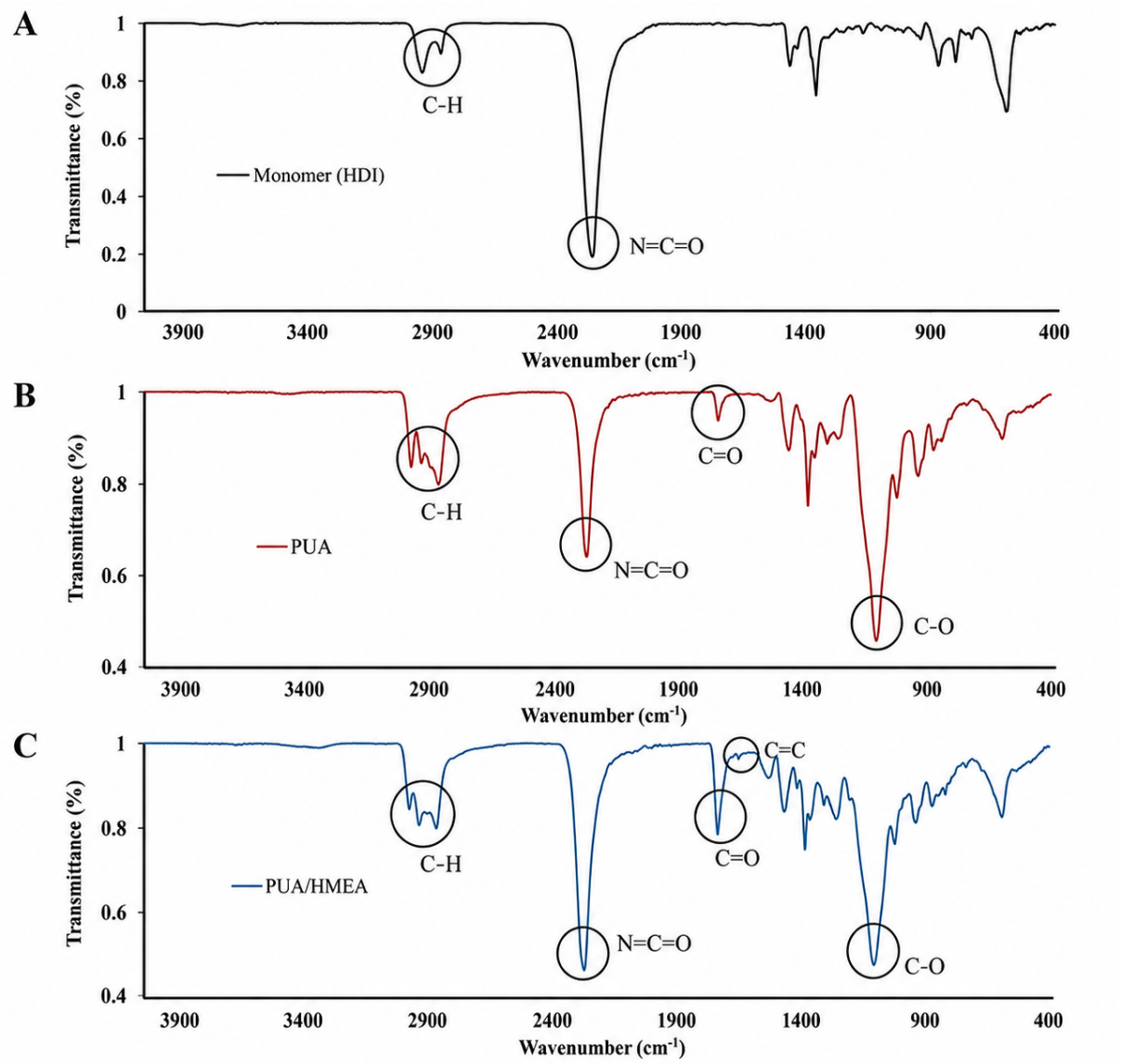

Figure 2 The FTIR spectra of HDI, neat PUA, and PUA/HMEA hybrid resins showed characteristic bands of NCO (~2251 cm^{-1}), carbonyl (1719 cm^{-1}), and C=C (~1644 cm^{-1}), confirming the incorporation of HMEA into the polyurethane network. Circled regions indicate characteristic functional-group absorption bands

3.2 Viscosity

Polymer viscosity is a key parameter in determining the suitability of the material for industrial applications. Excessively high viscosity can hinder application and processing, whereas very low viscosity may result in sagging or poor film build. Table 2 summarizes the influence of HMEA content on the viscosity and thixotropic behavior of PUA systems, measured at rotational speeds of 5 and 50 rpm.

At 5 rpm, the viscosity of neat PUA was 3492 mPa · s and decreased progressively with increasing HMEA content to 2560 mPa · s for PUA/3 HMEA, 1750 mPa · s for PUA/6 HMEA, and 620 mPa · s for PUA/12 HMEA. A similar trend was observed at 50 rpm, where the viscosity decreased from 3264 mPa · s for PUA to 1990, 1100, and 350 mPa · s for PUA/3 HMEA, PUA/6 HMEA, and PUA/12 HMEA, respectively. The marked decrease in viscosity with increasing HMEA content is attributed to dilution by a low-molecular-weight reactive monomer with reduced intermolecular chain entanglement. This behavior is advantageous for coating applications because it may improve the spreadability, substrate wetting, and ease of processing during film application. These reductions are attributed to the influence of HMEA on the soft segments of polyurethane, which are closely related to the polyol backbone. HMEA incorporation alters chain mobility and introduces additional hydroxyl functionality, leading to changes in the system's flow behavior.

The molecular structure of the soft segment derived from the polyol used to prepare the material also affects the rheological properties of polyurethane materials. In the current system, polyol materials of different molecular weights (GP-2000 and GP-4000) play an important role in controlling the polymer chains' flexibility and interchain interactions. The higher molecular weight of the GP-4000 chains enhances chain flexibility to a greater extent. The shorter chains of GP-2000 are beneficial for increasing the density of hydroxyl groups for crosslinking.

The thixotropic index (TI) was also strongly affected by the presence of HMEA, as shown in Table 2. The TI increased markedly from 1.06 for neat PUA to 1.59 for PUA/6 HMEA and to 1.77 for PUA/12 HMEA, indicating enhanced shear-thinning behavior with increasing HMEA content.

The formation of a transient microstructure within the hybrid polymer system can explain the increased thixotropic response. The addition of HMEA also adds functional groups capable of temporary intermolecular interactions, such as hydrogen bonding or physical entanglements. Under shear stress, these temporary intermolecular interactions are broken down, resulting in reduced viscosity. The microstructure also tends to re-establish itself once the shear stress is relieved. The effect of the polyol chain length and the addition of the HMEA on the shear-thinning response of the PUA/HMEA system was increased.

The observed decrease in viscosity with increasing HMEA content is consistent with previous studies on polyurethane acrylate hybrid systems, where the incorporation of low-molecular-weight acrylate monomers reduces intermolecular interactions and enhances chain mobility (Puyadena et al., 2022; Xu et al., 2012). Similar trends have been reported for hybrid coatings, in which increasing acrylate content leads to lower viscosity and improved processability, although excessive reduction may adversely affect film formation.

Furthermore, the increase in the thixotropic index with higher HMEA content agrees with previous reports indicating that hybrid polymer systems exhibit enhanced shear-thinning behavior due to the formation of reversible physical interactions, such as hydrogen bonding and chain entanglements (Shafeeq & Unnikrishnan, 2020). The relatively high thixotropy observed in this system improved application performance, particularly in coating processes where sagging resistance and good leveling behavior are required.

The marked decrease in viscosity with increasing HMEA content is attributed to dilution by a low-molecular-weight reactive monomer with reduced intermolecular chain entanglement. This behavior is advantageous for coating applications because it may improve the spreadability, substrate wetting, and ease of processing during film application (Wang & Soucek, 2013; Zvonkina & Hilt, 2015).

3.3 Adhesion

Polyurethane (PU) adheres to metal surfaces through physical adsorption and chemical bonding between its isocyanate groups and the metal substrate. The strength of this adhesion depends on several factors, including the isocyanate content, type of polyol used, and presence of acrylic polymers. Figure 3 shows how the addition of HMEA affects the adhesion of PU/HMEA hybrid resins to metal substrates. The results clearly demonstrate that incorporating HMEA into PUA significantly affects adhesion. For instance, pure PUA exhibited an adhesion strength of 3.2 MPa on metal. When HMEA was added, the adhesion improved noticeably: PUA containing 3% HMEA achieved 6.2 MPa, while PUA with 12% HMEA achieved the highest adhesion of 10.5 MPa. The observed enhancement is mainly due to the increased crosslinking between PUA and HMEA. The NCO and N–H groups, along with the double bonds present on the substrate, play a key role in strengthening this adhesion. Improved adhesion may also arise from enhanced substrate wetting before curing, followed by higher cohesive strength after curing due to increased crosslink density within the hybrid network (Parhizkar et al., 2018; Xu et al., 2024).

Table 2 Effect of HMEA content on the viscosity and thixotropic index of PUA and PUA/HMEA hybrids

Sample	5 rpm	50 rpm	TI
PUA	3492 ± 54	3264 ± 75	1.07 ± 0.01
PUA / 3 HMEA	2560 ± 81	1990 ± 72	1.29 ± 0.01
PUA / 6 HMEA	1750 ± 78	1100 ± 70	1.59 ± 0.06
PUA / 12 HMEA	620 ± 29	350 ± 20	1.77 ± 0.02

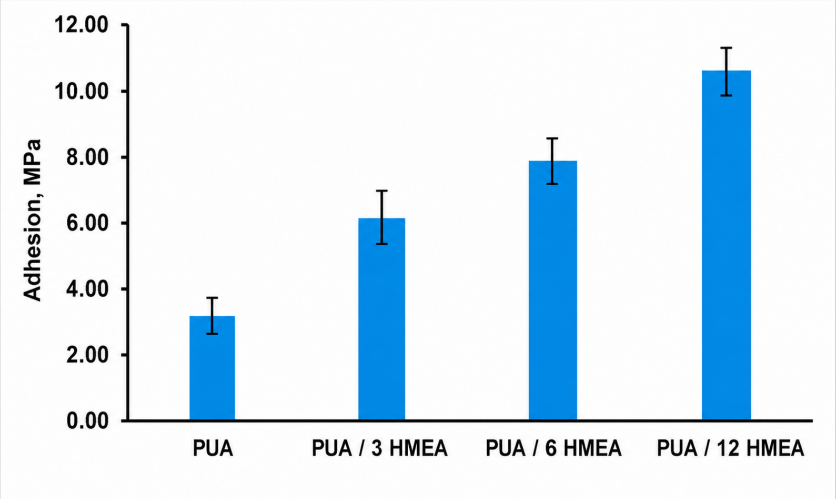

Figure 3 Pull-off adhesion strength of neat PUA and PUA/HMEA coatings on steel substrate as a function of HMEA content, showing progressive improvement in interfacial bonding with increasing HMEA loading

Polyurethane (PU) adheres to metal surfaces through physical adsorption and chemical bonding between its isocyanate groups and the metal substrate. The strength of this adhesion depends on several factors, including the isocyanate content, type of polyol used, and presence of acrylic polymers (Dillingham & Moriarty, 2003; Tardio et al., 2019).

3.4 Mechanical Properties

Several factors affect the chemical behavior of polymeric materials, including the type of monomer, overall composition, choice of solvent, temperature, degree of crosslinking, and concentration. Table 3 summarizes the effect of incorporating HMEA into the PUA matrix.

Table 3 Mechanical Characteristics of the PUA and PUA/HMEA Hybrid Materials

	Tensile strength (MPa)	Elongation (%)	Hardness (Shore D)	Contact angle (°)	Impact test	Cross Hatch
PUA	75 ± 4	200 ± 20	45 ± 1	105 ± 1	Pass	Pass
PUA/ 3 HMEA	127 ± 7	130 ± 13	57 ± 1	130 ± 3	Pass	Pass
PUA/ 6 HMEA	145 ± 9	105 ± 14	65 ± 1	139 ± 2	Pass	Pass
PUA/ 12 HMEA	205 ± 11	85 ± 9	74 ± 1	153 ± 2	Pass	Pass

The incorporation of HMEA into the PUA matrix to form hybrid materials resulted in enhanced tensile strength, surface hardness, and contact angle, while a decrease in elongation at break was observed. These mechanical performance enhancements of the PUA/HMEA hybrids are mainly attributed to the presence of double bonds and hydroxyl groups in HMEA, which promote hydrogen bonding between PUA and HMEA (Figure 1). Pure PUA exhibited a tensile strength of 75 MPa, which increased to 127 MPa for PUA/3 HMEA and to 205 MPa for PUA/12 HMEA. Similarly, the hardness (Shore D) increased from 45 for PUA to 74 for PUA/12 HMEA. All formulations successfully passed the impact and crosshatch adhesion tests. Overall, the PUA/HMEA hybrids exhibited superior mechanical performance compared with neat PUA, which can be attributed to the dual crosslinking interactions between PUA and HMEA, as shown in Figure 4. The tensile strength achieved in the present work (205 MPa) exceeds many previously reported polyurethane–acrylate systems, highlighting the effectiveness of the present formulation strategy based on an elevated NCO/OH ratio and a tailored hybrid network design (Lei et al., 2015).

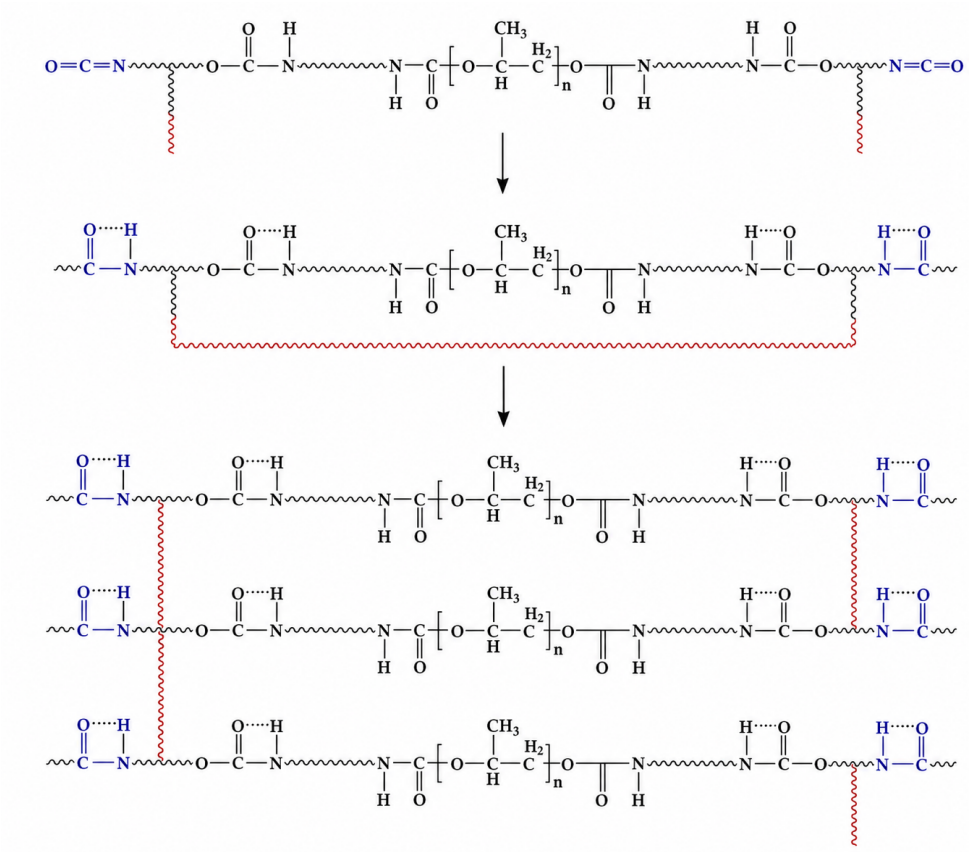

Figure 4 Schematic representation of additional crosslinking interactions introduced by HMEA within the PUA/HMEA hybrid network, contributing to enhanced mechanical strength and chemical resistance

3.5 Evaluation of Chemical and Corrosion Resistance

Table 4 illustrates how HMEA incorporation affects the chemical and corrosion resistance of PUA/HMEA hybrid coatings when exposed to solvents, acidic and alkaline media, water, and saturated conditions. The results show that polyurethane coatings possess good inherent resistance to alkaline solutions, water, and ethylene glycol. The introduction of HMEA into the PUA matrix further enhances both chemical stability and corrosion protection. In particular, the coating containing 3% HMEA exhibited satisfactory resistance to most chemical and corrosive environments, while the corrosion resistance was markedly improved by increasing the HMEA content to 12%. Overall, the PUA/HMEA formulation containing 12% HMEA exhibited the best chemical and corrosion resistance among the tested samples. The observed variations in corrosion resistance are primarily attributed to differences in the adhesion strength between the coating and the metal surface (Ito et al., 2019; Kozakiewicz, 2015; Madbouly, 2021; Negim et al., 2020).

Morphological characterization methods such as scanning electron microscopy (SEM) can provide valuable information on the degradation of the coating surfaces to further assess the stability of the coating surface following exposure to severe chemical environments. Although the SEM analysis of the coating surfaces is not considered a part of the current study, such morphological characterization methods can provide visual evidence on the morphological stability of the PUA/HMEA hybrid coating surfaces following corrosion testing. Further SEM characterization of the corrosion performance of the coatings is necessary to provide a better understanding of the relationship between the microstructural integrity of the coatings.

Table 4 The resistance of the hybrid films to chemical attack and corrosion progressively improved with increasing HMEA loading. (✓ = Suitable; ∼ = Swelling behavior; × = Not suitable)

Medium	PUA	PUA/HMEA-3	PUA/HMEA-6	PUA/HMEA-12
NaCl (10%)	O	O	O	O
NaOH (10%)	O	O	O	O
HCl (37%)	O	O	O	O
H_2SO_4 (37%)	Δ	Δ	O	O
Water	O	O	O	O
MEK	Δ	Δ	O	O
Xylene	O	O	O	O
Ethanol (20%)	O	O	O	O
Ethylene glycol	O	O	O	O
Wine	Δ	O	O	O
Acetone	Δ	O	O	O
Butyl alcohol	Δ	Δ	O	O

The improved chemical and solvent resistance observed for the hybrid coatings can also be attributed to the increased crosslink density of the PUA/HMEA network. A higher degree of crosslinking generally restricts polymer chain mobility and reduces the penetration of solvent molecules into the polymer matrix, thereby limiting swelling and improving the coating's barrier properties.

Although quantitative swelling measurements in organic solvents were not performed in the present study, the resistance behavior observed in the immersion tests suggests that the incorporation of HMEA contributes to the formation of a denser polymer network that effectively suppresses solvent-induced swelling and enhances the coating system's overall chemical stability.

Future work will focus on evaluating the swelling behavior of these hybrid coatings in various organic solvents to further elucidate the relationship between the network structure, solvent diffusion, and long-term chemical resistance performance.

The performance of the developed PUA/HMEA hybrid system was further evaluated by

comparing the results obtained with previously reported polyurethane acrylate materials. As summarized in Table 3, the tensile strength achieved in this study (up to 205 MPa) is significantly higher than many reported values for similar hybrid systems, which typically range between 50–150 MPa (Shafeeq & Unnikrishnan, 2020; Zhang et al., 2010). Similarly, the adhesion strength (10.5 MPa) and high contact angle values indicate superior interfacial bonding and surface hydrophobicity compared with conventional systems.

These enhanced properties can be attributed to the combined effect of a high NCO/OH ratio and optimized polyol composition, which promote higher crosslink density and improved network integrity. Overall, the results demonstrate that the proposed system exhibits competitive or superior performance compared with previously reported polyurethane–acrylate hybrid coatings. These improvements can be attributed to the combined effect of a high NCO/OH ratio and optimized polyol composition, which enhance crosslink density and overall network integrity.

4. Conclusions

Polyurethane–acrylate (PUA/HMEA) hybrid coatings were successfully developed using a relatively high NCO/OH ratio (2.5) combined with a tailored polyol composition. The incorporation of HMEA significantly enhanced the performance of the polyurethane matrix through the formation of a densely crosslinked network, leading to improved mechanical strength, adhesion, and surface properties. The optimized formulation (PUA/HMEA-12) exhibited a tensile strength of 205 MPa, an adhesion strength of 10.5 MPa, and a contact angle of 153°, along with excellent resistance to water and solvents. These improvements are attributed to the increased crosslink density and stronger intermolecular interactions within the hybrid system, although the elongation at break was reduced due to the increased rigidity. Overall, this study demonstrates that controlling the NCO/OH ratio and polyol architecture, together with acrylate incorporation, is an effective strategy for tailoring structure–property relationships in polyurethane–acrylate hybrids for high-performance coating applications. Future work will focus on further optimizing the balance between strength and flexibility and investigating the coatings' long-term durability, swelling behavior, and microstructural characteristics under aggressive environmental conditions.

Data Availability Statement

Data will be available on request from the corresponding author.

Conflict of Interest

The authors declare no conflicts of interest.

References

Aizpurua, J., Martin, L., Fernández, M., González, A., & Irusta, L. (2020). Recyclable and healing polyurethane/acrylic coatings from uv-curable waterborne dispersions. *Progress in Organic Coatings*, *139*, 105460. https://doi.org/10.1016/j.porgcoat.2019.105460

Allami, T., Alamiery, A., Nassir, M. H., & Kadhum, A. H. (2021). Investigating physio-thermo-mechanical properties of polyurethane and thermoplastics nanocomposite in various applications. *Polymers*, *13*(15), 2467. https://doi.org/10.3390/polym13152467

Amini, G., Motiei Shahreza, S., Raouffard, A., Kalali, E. N., & Mohammadi, A. (2025). Tannic acid-enriched polyurethanes: Synthesis, properties, and application potential. *Industrial Crops and Products*, *236*, 122027. https://doi.org/10.1016/j.indcrop.2025.122027

Asensio, M., Ferrer, J.-F., Nohales, A., Culebras, M., & Gómez, C. M. (2023). The role of diisocyanate structure to modify properties of segmented polyurethanes. *Materials*, *16*(4), 1633. https://doi.org/10.3390/ma16041633

Azani, M.-R., & Hassanpour, A. (2024). UV-Curable Polymer Nanocomposites: Material Selection, Formulations, and Recent Advances. *Journal of Composites Science*, *8*, 441. https://doi.org/10.3390/jcs8110441

Breheny, C., Colbert, D. M., Bezerra, G., Geever, J., & Geever, L. M. (2025). Evaluating the chemical resistance and performance of thermochromic polymers for food packaging. *Materials*, *18*(9), 2085. https://doi.org/10.3390/ma18092085

Byczyński, Ł., Mariusz, S., & Maciej, K. (2024). Poly(urethane-acrylate) cationomer coatings with increased hydrophobicity and reduced flammability. *Progress in Organic Coatings*, *186*, 108008. https://doi.org/10.1016/j.porgcoat.2023.108008

Dall'Agnol, L., Dias, F. T. G., Ornaghi Jr., H. L., Sangermano, M., & Bianchi, O. (2021). UV-curable waterborne polyurethane coatings: A state-of-the-art and recent advances review. https://doi.org/10.1016/j.porgcoat.2021.106156

David, W., Thomas, G., Stuart, L. C., & Daniel, E. H. (2023). An overview of polyurethane biomaterials and their use in drug delivery. *Journal of Controlled Release*, *363*, 376–388. https://doi.org/10.1016/j.jconrel.2023.09.036

Dillingham, R. G., & Moriarty, C. (2003). The adhesion of isocyanate-based polymers to steel. *The Journal of Adhesion*, *79*(3), 269–285. https://doi.org/10.1080/00218460309554

Guo, G., You, T., Yang, X., & Li, W. (2024). Ultraviolet-cured polyurea–polyurethane acrylate/polysiloxane hybrid anti-fouling coatings. *Progress in Organic Coatings*, *197*, 108832. https://doi.org/10.1016/j.porgcoat.2024.108832

Ito, N. M., Gouveia, J. R., Vidotti, S. E., Ferreira, M. C. G. C., & Santos, D. J. (2019). Interplay of polyurethane mechanical properties and adhesion. *The Journal of Adhesion*, *96*(14), 1219–1232. https://doi.org/10.1080/00218464.2019.1580580

Keskin, S., Cheaburu-Yilmaz, C. N., Altinisik Tagac, A., Darie-Nita, R. N., & Yilmaz, O. (2025). Synthesis of acrylic–urethane hybrid polymer dispersions and investigations on their properties as binders in leather finishing. *Polymers*, *17*(3), 308. https://doi.org/10.3390/polym17030308

Kim, G. B., Guo, J., Hu, J., Shan, D., & Yang, J. (2016). Novel applications of urethane/urea chemistry in the field of biomaterials. In *Advances in polyurethane biomaterials* (pp. 115–147). Elsevier. https://doi.org/10.1016/b978-0-08-100614-6.00004-4

Kim, T. H., Kim, H. S., & Lee, S.-H. (2026). Sustainable polyurethane systems: Integrating green synthesis and closed-loop recovery. *Polymers*, *18*(2), 246. https://doi.org/10.3390/polym18020246

Kozakiewicz, J. (2015). Developments in aqueous polyurethane and polyurethane-acrylic dispersion technology. Part I. *Polimery*, *60*(9), 525–535. https://doi.org/10.14314/polimery.2015.525

Kozakiewicz, J. (2016). Developments in aqueous polyurethane and polyurethane-acrylic dispersion technology. Part II. *Polimery*, *61*(2), 81–91. https://doi.org/10.14314/polimery.2016.081

Lei, L., Xia, Z., Ou, C., Zhang, L., & Zhong, L. (2015). Effects of crosslinking on adhesion behavior of waterborne polyurethane ink binder. *Progress in Organic Coatings*, *88*, 155–163. https://doi.org/10.1016/j.porgcoat.2015.07.002

Liu, D., Huyan, C., Li, H., Ge, J., Chen, F., & Zhang, L. (2026). Recycling and upcycling of polyurethane thermosets: The second life of polymers [In press]. *Advanced Materials*. https://doi.org/10.1002/adma.202515809

Maamoun, A. A., Arafa, M., & Esawi, A. M. K. (2025). Flexible polyurethane foam: Materials, synthesis, recycling, and applications in energy harvesting – a review. *Materials Advances*, *6*(6), 1842–1858. https://doi.org/10.1039/d4ma01026d

Madbouly, S. A. (2021). Waterborne polyurethane dispersions and thin films: Biodegradation and antimicrobial behaviors. *Molecules*, *26*(4), 961. https://doi.org/10.3390/molecules26040961

Manas, C. (2024). Compatibilization phenomenon in polymer science and technology: Chemical aspects. *Advanced Industrial and Engineering Polymer Research*, *7*, 363–372. https://doi.org/10.1016/j.aiepr.2024.01.002

Maurya, A. K., de Souza, F. M., & Gupta, R. K. (2023). Polyurethane and its composites: Synthesis to application. In *Acs symposium series* (pp. 1–20). American Chemical Society. https://doi.org/10.1021/bk-2023-1452.ch001

Negim, E., Shalash, M., Al Azzam, K. M., Sagatbekovna, M. Z., Kairatovna, B. A., Konstantinovich, A. T., Adlikhanovna, N. A., Ermekovna, K. A., & Ravindran, B. (2024a). Synthesis, characterization, and application of polyurethane-acrylic hybrids as anticorrosion coatings. *International Journal of Technology*, *15*(6), 2009–2023. https://doi.org/10.14716/ijtech.v15i6.7044

Negim, E.-S., Omurbekova, K., Bekbayeva, L., & Abdelhafiz, A. (2020). Effect of NCO/OH ratio on polyurethane–polyurea coatings. *Egyptian Journal of Chemistry*, *63*, 1–12. https://doi.org/10.21608/ejchem.2020.23845.2416

Negim, E.-S., Shalash, M., Mukatayeva, Z., Baidullayeva, A., Alferov, T., Nurtazina, A., Karabayeva, A., & Samy, M. (2024b). Mini review polyurethane hybrids: Preparation, characterization and applications. *Kompleksnoe Ispolzovanie Mineralnogo Syra = Complex Use of Mineral Resources*, *333*, 16–26. https://doi.org/10.31643/2025/6445.13

Niu, Z., & Bian, F. (2012). Synthesis and characterization of multiple cross-linking UV-curable waterborne polyurethane dispersions. *Iranian Polymer Journal*, *21*(4), 221–228. https://doi.org/10.1007/s13726-012-0021-6

Oladele, I. O., Oki, V. O., Omotosho, T. F., Adebanjo, M. B., Ayanleye, O. T., & Adekola, S. A. (2025). Sustainable polymer and polymer-based composite materials for extreme conditions and demanding applications – a review on pushing boundaries in materials science. *Next Materials*, *8*, 100775. https://doi.org/10.1016/j.nxmate.2025.100775

Parhizkar, N., Ramezanzadeh, B., & Shahrabi, T. (2018). Corrosion protection of epoxy coatings modified with graphene oxide. *Applied Surface Science*, *439*, 45–59. https://doi.org/10.1016/j.apsusc.2017.12.240

Peruzzo, P. J., Anbinder, P. S., Pardini, O. R., Costa, C. A., Galembeck, F., & Amalvy, J. I. (2010). Polyurethane/acrylate hybrids: Effects of acrylic content. *Journal of Applied Polymer Science*, *116*(5), 2694–2705. https://doi.org/10.1002/app.31795

Peruzzo, P. J., Anbinder, P. S., Pardini, O. R., Vega, J., Costa, C. A., Galembeck, F., & Amalvy, J. I. (2011). Waterborne polyurethane/acrylate: Comparison of hybrid and blend systems. *Progress in Organic Coatings*, *72*(3), 429–437. https://doi.org/10.1016/j.porgcoat.2011.05.016

Pooneh, K., & Reza, A. (2026). Advances and future directions in eco-friendly coatings: From chemistry to industrial applications. *Progress in Organic Coatings*, *214*, 110068. https://doi.org/10.1016/j.porgcoat.2026.110068

Puyadena, M., Etxeberria, I., Martin, L., Mugica, A., Agirre, A., Cobos, M., Gonzalez, A., Barrio, A., & Irusta, L. (2022). Polyurethane/acrylic hybrid dispersions containing phosphorus reactive flame retardants as transparent coatings for wood. *Progress in Organic Coatings*, *170*, 107005. https://doi.org/10.1016/j.porgcoat.2022.107005

Shafeeq, V., & Unnikrishnan, G. (2020). Experimental and theoretical evaluation of mechanical, thermal and morphological features of EVA-millable polyurethane blends. *Journal of Polymer Research*, *27*, 1–11. https://doi.org/10.1007/s10965-020-2027-7

Shimin, G., Zhen, H., Yizhen, C., Ying, L., Liyuan, Z., Mingen, F., Renhui, Q., & Wendi, L. (2024). Polyurethane acrylate covalent adaptable networks based on the autocatalytic effect of palm oil-based diol. *ACS Applied Polymer Materials*, *6*(23), 14760–14771. https://doi.org/10.1021/acsapm.4c02964

Shuang, W., Shaoping, M., Qinghua, Z., & Chao, Y. (2025). A comprehensive review of polyurethane: Properties, applications and future perspectives. *Polymer*, *327*, 128361. https://doi.org/10.1016/j.polymer.2025.128361

Son, S., Kim, K., Lee, Y., Lee, D., & Kim, H. (2011). Effect of acrylic monomer content on properties of waterborne polyurethane/acrylic hybrids. *Journal of Applied Polymer Science*, *124*(6), 5113–5121. https://doi.org/10.1002/app.35662

Su, Y., Chen, Y., Zhang, H., Liu, S., & Guo, P. (2024). Synergistic enhancement effect of multi-dimensional nanomaterials on high-damping polyurethane. *Journal of Rubber Research*, *28*, 39–50. https://doi.org/10.1007/s42464-024-00275-1

Suwen, Z., Yaxuan, W., Dunjie, F., Chaoxia, W., & Yunjie, Y. (2022). Synthesis of branched waterborne polyurethane and its application in the preparation of liquid indigo dispersion. *Progress in Organic Coatings*, *171*, 107021. https://doi.org/10.1016/j.porgcoat.2022.107021

Tardio, S., Abel, M.-L., Carr, R. H., & Watts, J. F. (2019). The interfacial interaction between isocyanate and stainless steel. *International Journal of Adhesion and Adhesives*, *88*, 1–10. https://doi.org/10.1016/j.ijadhadh.2018.10.008

Wang, X., & Soucek, M. D. (2013). Investigation of non-isocyanate urethane dimethacrylate reactive diluents for UV-curable polyurethane coatings. *Progress in Organic Coatings*, *76*(7–8), 1057–1067. https://doi.org/10.1016/j.porgcoat.2013.03.001

Xu, H., Qiu, F., Wang, Y., Wu, W., Yang, D., & Guo, Q. (2012). UV-curable waterborne polyurethane-acrylate. *Progress in Organic Coatings*, *73*(1), 47–53. https://doi.org/10.1016/j.porgcoat.2011.08.019

Xu, H., Zhang, X., Yu, Y., Yu, Y., & Weng, L. (2024). Enhanced adhesion of epoxy resin composites. *Next Materials*, *3*, 100072. https://doi.org/10.1016/j.nxmate.2023.100072

Zhang, T., Wu, W., Wang, X., & Mu, Y. (2010). Effect of average functionality on properties of UV-curable waterborne polyurethane-acrylate. *Progress in Organic Coatings*, *68*(3), 201–207. https://doi.org/10.1016/j.porgcoat.2010.02.004

Zhang, Z., Ni, N., & Xu, Y. (2025). Effects of different polyols with functions on the properties of polyester polyol-based polyurethane coatings. *Coatings*, *15*(1), 61. https://doi.org/10.3390/coatings15010061

Zhou, J., Luo, F., Tang, L., & Guo, Z. (2024). Fabrication of polyurethane–polyacrylate hybrid latexes with high organosilicon content via phase inversion emulsion polymerization. *Molecules*, *29*(24), 5870. https://doi.org/10.3390/molecules29245870

Zvonkina, I. J., & Hilt, M. (2015). Tuning the mechanical performance and adhesion of polyurethane UV-cured coatings by composition of acrylic reactive diluents. *Progress in Organic Coatings*, *89*, 288–296. https://doi.org/10.1016/j.porgcoat.2015.08.006